**Supporting Information**

# Achieving Highly Efficient, Selective and Stable $CO_2$ Reduction on Nitrogen Doped Carbon Nanotubes

Jingjie Wu[1], Ram Manohar Yadav[1], Mingjie Liu[1], Pranav P. Sharma[2], Chandra Sekhar Tiwary[3], Lulu Ma[1], Xiaolong Zou[1], Xiao-Dong Zhou[2*], Boris I. Yakobson[1], Jun Lou[1*] and Pulickel M. Ajayan[1]*

[1]Department of Material Science and NanoEngineering, Rice University, Houston, TX 77005, USA, [2]Department of Chemical Engineering, University of South Carolina, Columbia, SC 29201, USA, [3]Department of Materials Engineering, Indian Institute of Science, Bangalore 560012, India.

Correspondence: zhox@rice.edu (X. D. Zhou), jlou@rice.edu (J. Lou) and ajayan@rice.edu (P. M. Ajayan)

## Materials

$KHCO_3$ (99.7%), Nafion perfluorinated resin solution (5 wt.%) and isopropanol (99.5%) were purchased from Sigma-Aldrich; hydrogen (99.999%), argon (99.999%), helium (99.999%), and carbon dioxide (99.999%) were purchased from Airgas; Nafion® 212 membrane was purchased from Dupont; Pt/C (60%) was obtained from Johnson Matthey; Ag powder (APS 20-40 nm), Au powder (ASP 500-800 nm), Cu powder (APS 200-300nm) and Zn powder (6 μm) were purchased from Alfa Aesar. The graphite gas diffusion layer (GDL 10 BC) was ordered from SGL group. All chemicals were used without further purification. Electrolyte solutions were prepared with DI water (Siemens, Labstar).

## Electrode preparation

The N-doped carbon nanotubes (NCNTs) gas diffusion electrodes (NCNTs GDEs) were prepared from the NCNT arrays. In short, a suspension of NCNTs array particles and Nafion perfluorinated resin solution along with a 50/50 mixture of water and isopropanol were formed by ultrasonicating for at least 30 min before being sprayed onto GDLs to form GDEs with a NCNTs loading of 0.3~0.5 mg $cm^{-2}$. The NCNTs GDEs were then heat-treated at 130 $^{oC}$ for 30

min in the vacuum oven and allowed to cool slowly back to room temperature before testing. The other metals (Cu, Zn, Au and Ag) based GDEs followed the same preparation precedure and their loadings were ~ 1.5 mg $cm^{-2}$. The anode, Pt GDE, with a Pt loading of 0.3 mg $cm^{-2}$ was made as the similar procedure as NCNTs GDE. The Pt GDE was hot-pressed at 130 $^{o}$C and 50 PSI for 5 min with a Nafion® 212 membrane which prevents CO diffusing to Pt anode.

**Calibration of anode potential for $H_2$ oxidation on Pt GDE**

The potential of $H_2$ oxidation on Pt GDE was measured in a half cell with a three-electrode setup. The setup can be found in our previous publication.[1] The Pt GDE hot pressed with a Nafion membrane serves as the working electrode, a Pt foil with big area (2 × 2 cm) was used as the anode. A Ag/AgCl with saturated KCl was employed as the referece electrode. The potential was later re-scaled to reversible hydrogen elecrtrode, $E_{RHE} = E_{Ag/AgCl} + 0.20 + 0.0591pH$. The electrolyte was 0.1 M $KHCO_3$ the same as that in the $CO_2$ reduction. Constant current up to 25 mA $cm^{-2}$ was applied for 30 min and the E-t curve was recorded.

**DFT calculations**

All calculations were performed through density functional theory (DFT) implemented in Vienna Ab-initio Simulation Package (VASP)[2, 3] with Perdew, Burke and Ernzerhof functional[4]. The (5, 5) single-walled carbon nanotubes (CNTs) with 5 unit cell as well as three different N-bond types, including graphitic, pyridinic and pyrrolic N, were chosen as our models. In the aperiodic directions a vacuum layer of 11 Å was selected to keep the interaction between periodic images of the system negligible. Full structural relaxation with K-point mesh 1×1×3 was performed until all forces were less than 0.01 eV/Å. The ground state structures of COOH* and CO* adsorbed on CNT/NCNT were determined by searching different possible configurations to find

the one with the lowest energy. The ground state structures of the intermediate states (COOH* on CNT/NCNT) are shown in Fig.S12.

**Free Energy diagram based on CHE**

The free energy changes at each electrochemical step involving an proton-electron transfer were computed based on computational hydrogen electrode (CHE) model[5], in which the zero voltage (vs. RHE) is defined in the equilibrium of $H^+ + e^- \leftrightarrow \frac{1}{2}H_2\ (g)$ at all pH, temperature and $H_2$ pressure of 1 atm. The chemical potential of the proton-electron pairs can be calculated as a function of applied voltage as $\mu(H^+) + \mu(e^-) = \frac{1}{2}\mu(H_{2(g)}) - eU$. The free energy of adsorbates and non-adsorbed gas-phase molecules is calculated as $G = E_{elec} + E_{ZPE} + \int C_P dT - TS$. The $E_{elec}$ is the electronic energy calculated by DFT; $E_{ZPE}$ is the zero point energy estimated under harmonic approximation by taking the vibrational frequencies of adsorbates or molecules as calculated within DFT. The $\int C_P dT$ and $TS$ are small for the adsorbates compared to $E_{elec}$ and $E_{ZPE}$, and thus neglected in this study for adsorbates. The entropies of $H_2$ (g), $CO_2$ (g) and CO (g) at 1 atm are used, while the entropy of $H_2O$ (l) is calculated at 0.035 atm, which corresponds to the vapor pressure of liquid water at 300 K. A correction of -0.51 eV for non-adsorbed gas-phase CO molecule has to be made due to the use of PBE functional.[6] The solvation effect has been included for COOH* and CO* by stabilizing 0.25 eV and 0.1 eV respectively.[6] The free energies of $CO_2$, CO, $H_2O$ and $H_2$ are listed in Table S2.

**The binding energy of COOH* and CO***

The binding energies for COOH* and CO* on pure and N-doped CNTs are calculated by $E_b = E(A^*) - E(tube) - xE_{f,C} - yE_{f,O} - zE_{f,H}$. $E(A^*)$ is the total energy of the tube with attached adsorbates. $E(tube)$ is the energy of pure or N-doped CNT. *x, y* and *z* are the numbers

of C, O and H in the adsorbates. $E_f$ is the formation energies of C, O and H which are calculated by linear combinations of electronic energies of gas-phase CO, $H_2O$ and $H_2$.

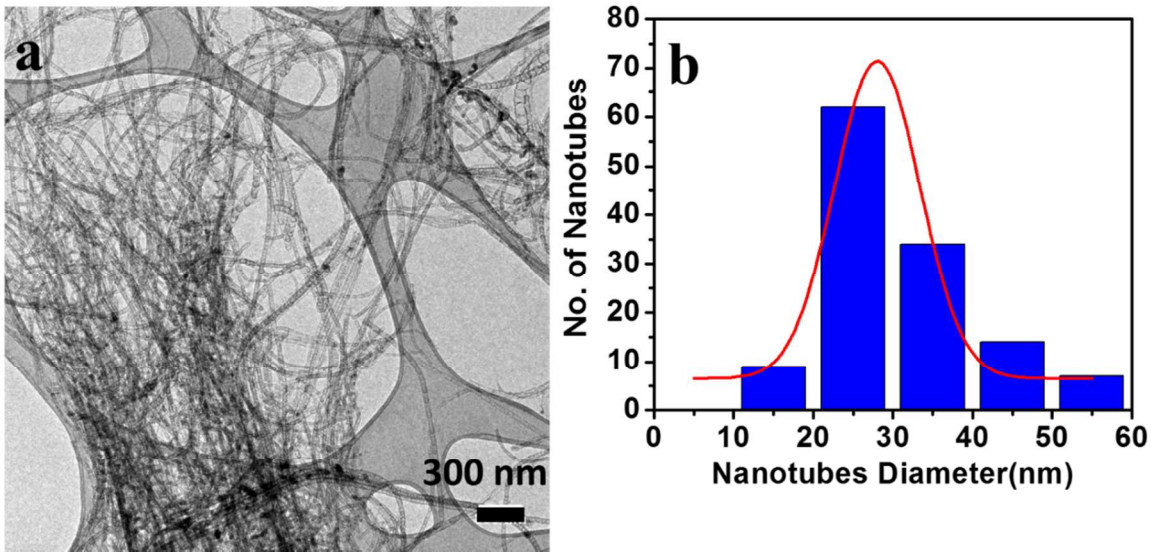


Figure S1. TEM characterization of NCNTs. (a) Low magnification images of NCNTs and (b) the corresponding tube diameter distribution.

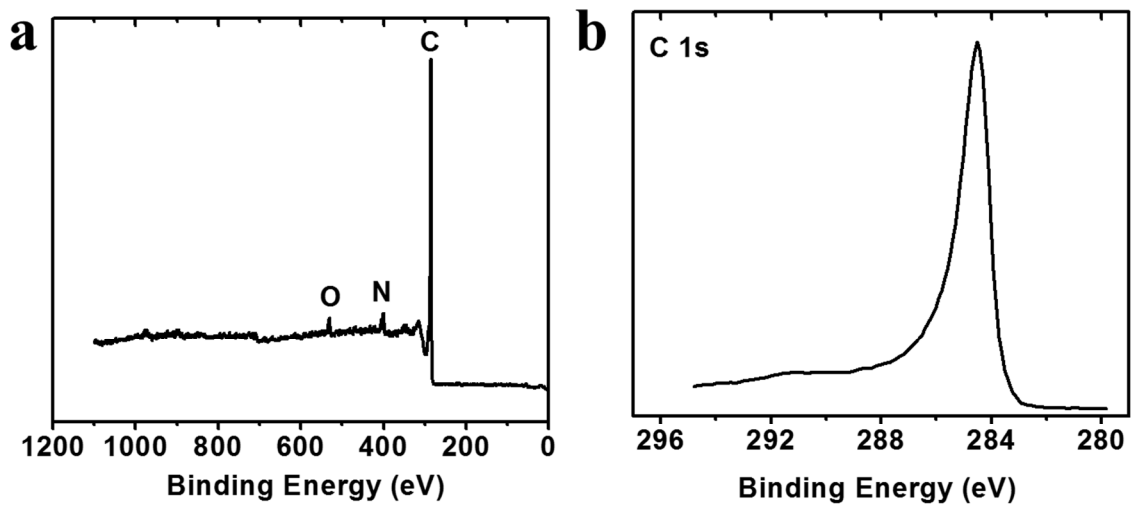


Figure S2. XPS characterization of NCNTs. (a) Survey scan of NCNTs showing C, N and O three elements. (b) Fine scan of C 1s.

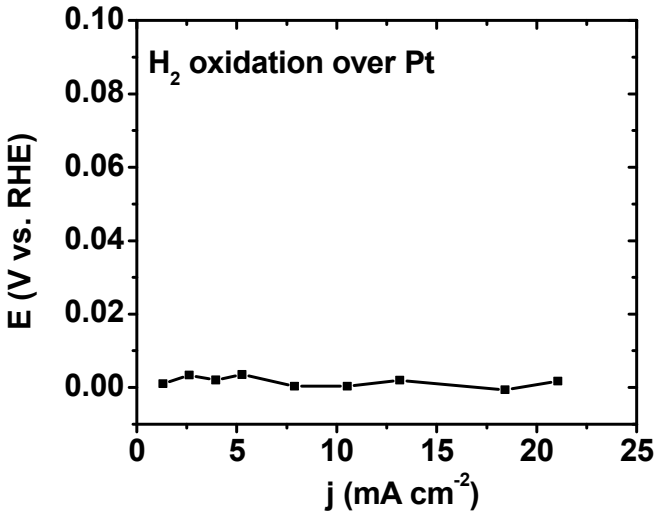


Figure S3. The dependence of potential for $H_2$ oxidation on Pt GDE on the current densities. The overpotential for $H_2$ oxidation on Pt electrode is negligible at the studied current density range.

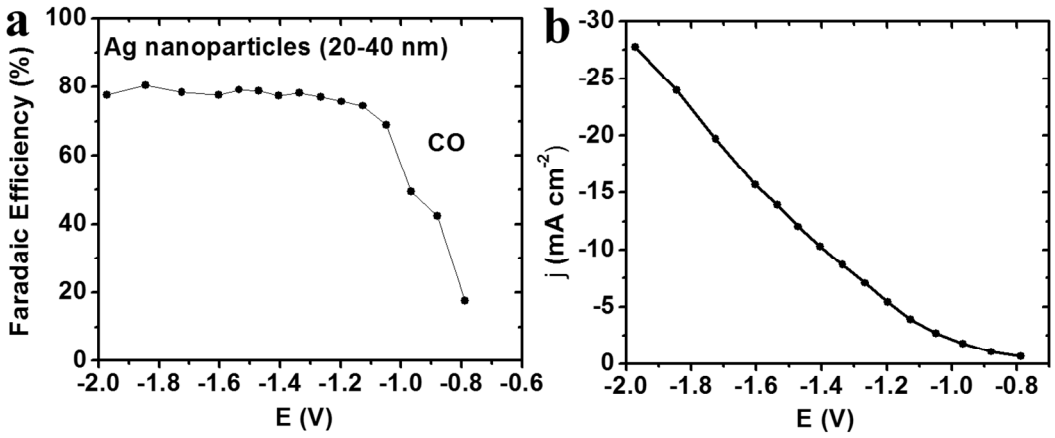


Figure S4. Electrochemical activity of Au powder to $CO_2$ reduction. (a) Faradaic efficiency of CO, and (b) total current density at each tested cell voltage.

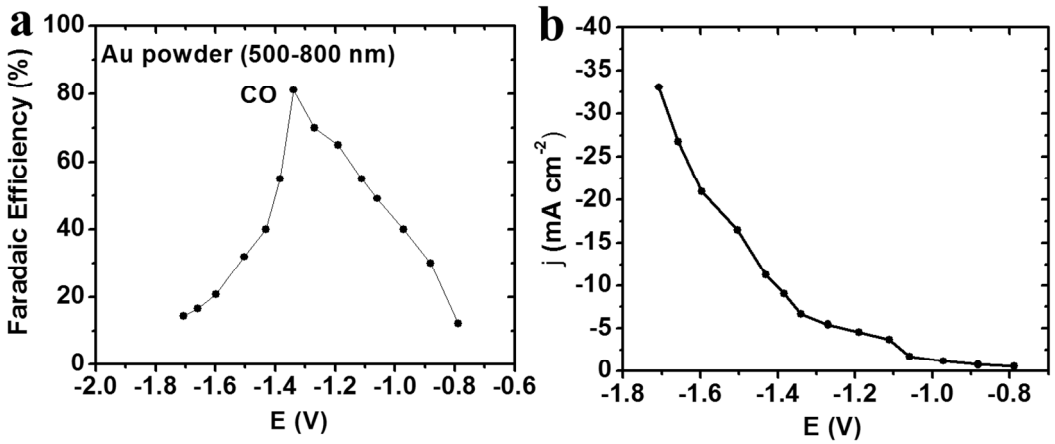


Figure S5. Electrochemical activity of Ag nanoparticles to $CO_2$ reduction. (a) Faradaic efficiency of CO, and (b) total current density at each tested cell voltage.

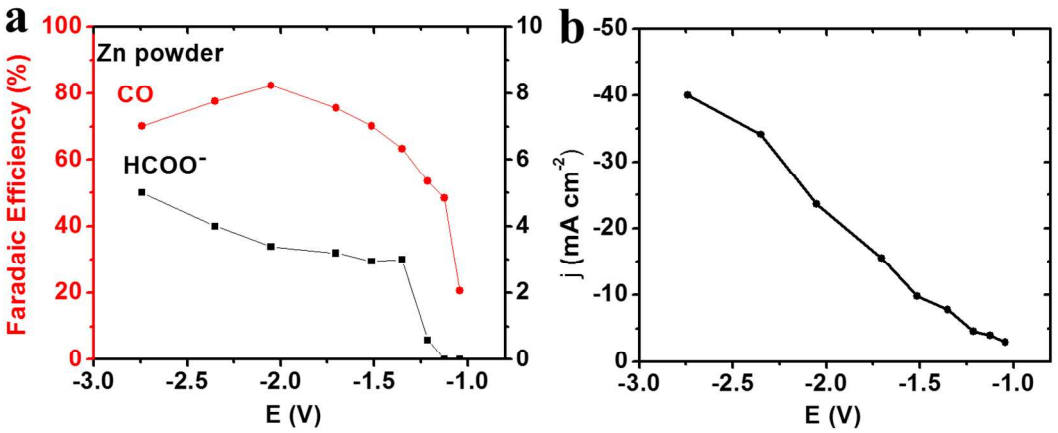


Figure S6. Electrochemical activity of Zn powder to $CO_2$ reduction. (a) Faradaic efficiency of CO and formate, and (b) total current density at each tested cell voltage.

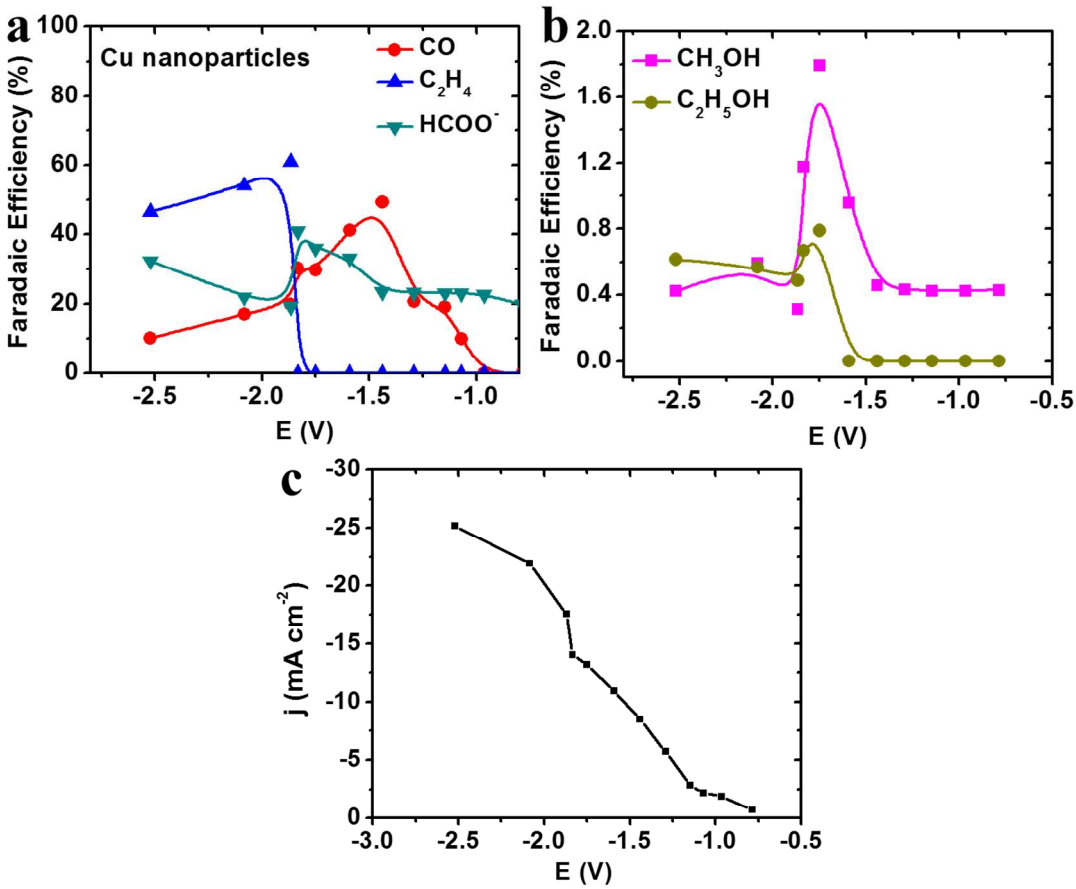


Figure S7. Electrochemical activity of Cu nanoparticles to $CO_2$ reduction. (a) Faradaic efficiency of CO, formate and $C_2H_4$, (b) Faradaic efficiency of $CH_3OH$ and $C_2H_5OH$, and (b) total current density at each tested cell voltage.

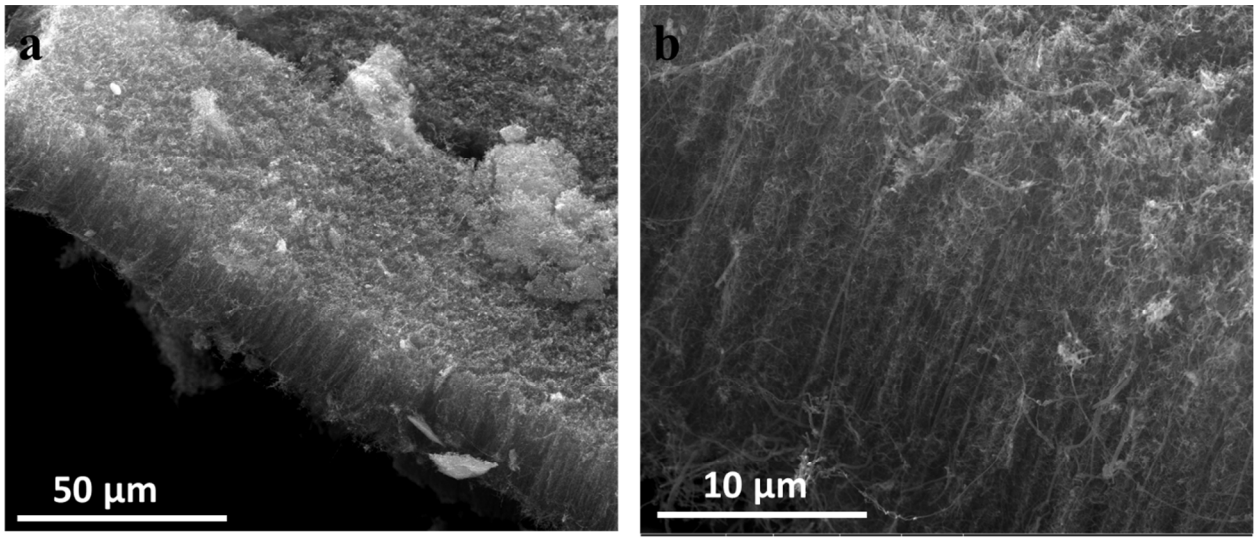


Figure S8. SEM images of pure CNTs. (a) A low magnification image showing the CNT arrays. (b) A high magnification image.

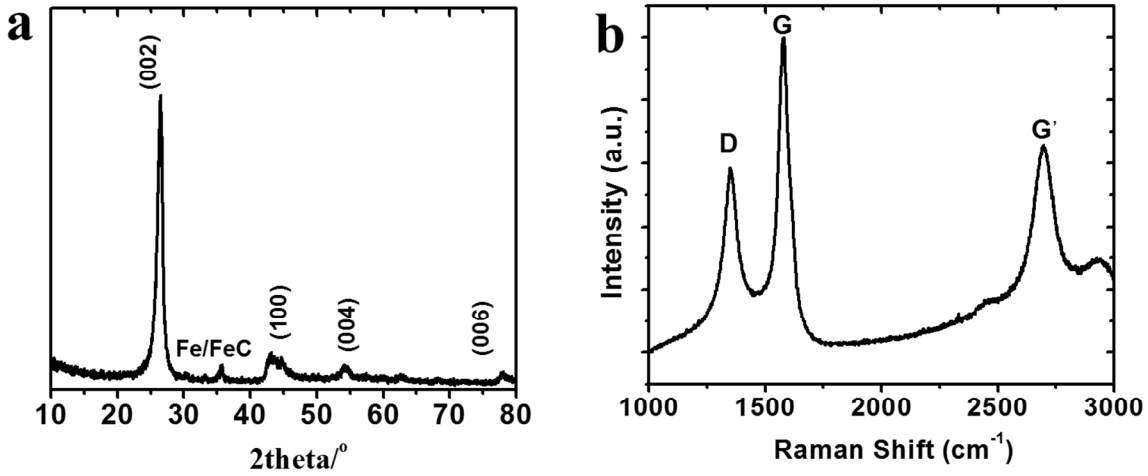


Figure S9. Microstructure characterization of pure CNTs. (a) XRD showing the same peak diffraction as NCNTs. A small diffraction peak assigned to iron species was observed. (b) Raman spectrum. The $I_d/I_g$ is 0.58.

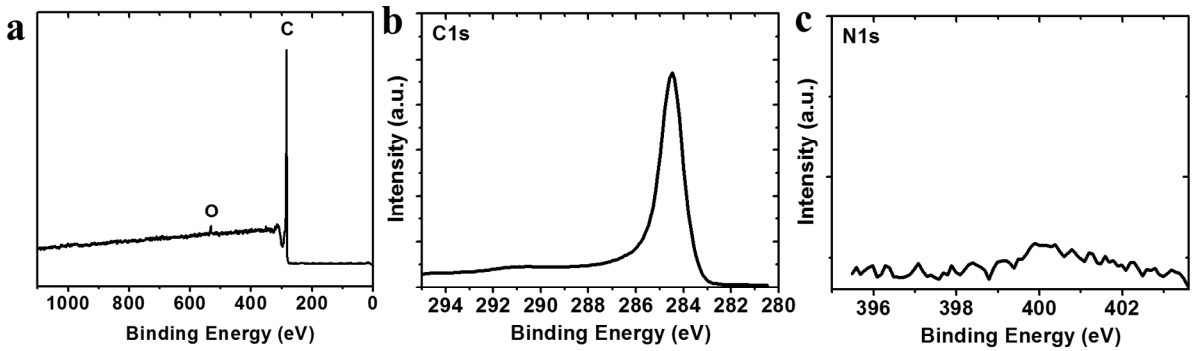


Figure S10. Chemical composition characterization of pure CNTs by XPS. (a) A survey scan, (b) fine scan of C 1s and (c) fine scan of N 1s showing the N content is under the detection limit of XPS.

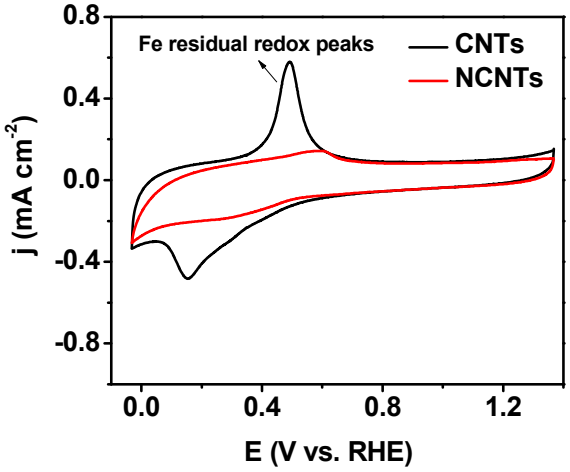


Figure S11. Cyclic voltammetry of NCNTs and CNTs in the electrolyte of 0.1 M KOH saturated with Ar. Scan rate: 50 mV $s^{-1}$. The 0.1 M KOH was used for the convenience of locating the Fe residual redox peaks as compared to the literatures.

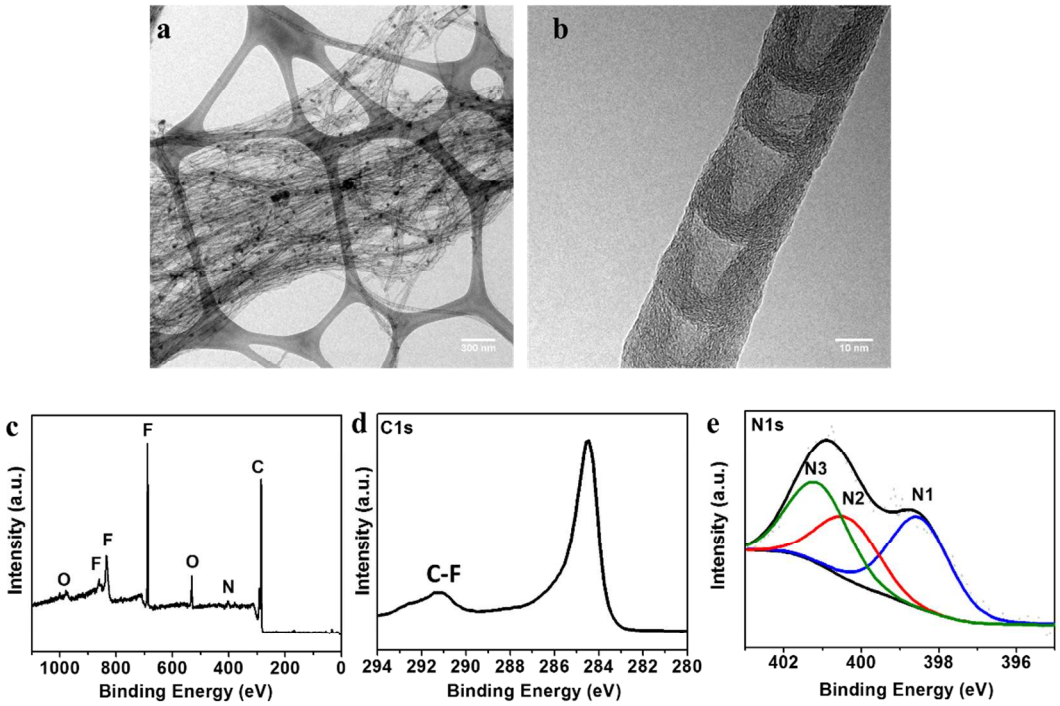


Figure S12. Physical characterization of NCNTs after long-term $CO_2$ reduction. (a) Low magnification TEM images, (b) a high magnification TEM image of single NCNT, (c) survey spectrum of XPS, the F coming from the Nafion binder, (d) and (e) fine scan of C1s and N1s, respectively.

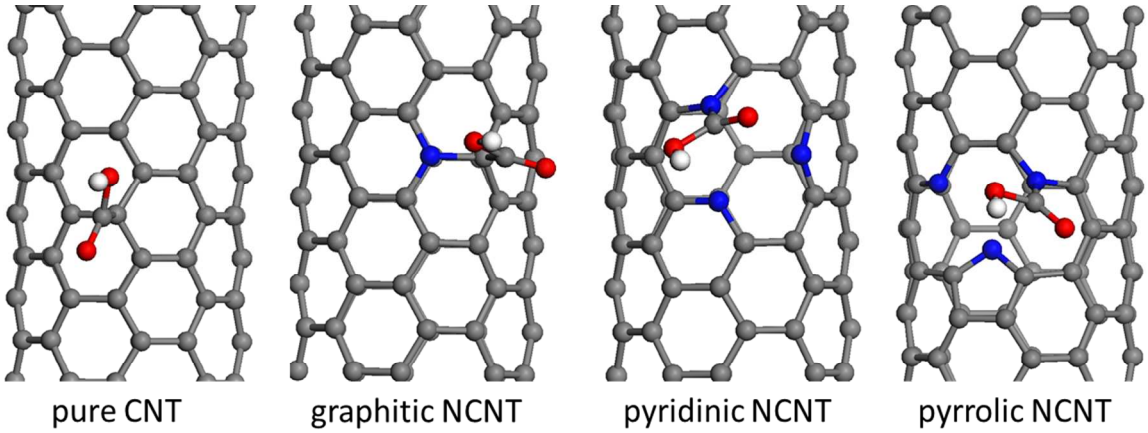


Figure S13. The ground state structure of COOH* adsorbed on pure CNT, graphitic N-doped CNT, pyridinic N-doped CNT and pyrrolic N-doped CNT. C, N, O and H atoms are represented by grey, blue, red and white spheres.

**Table S1.** Kinetic data of NCNTs, Au and Ag for electroreduction of $CO_2$ to CO.

| Material | Tafel Slope ( mV/dec) | $j_o$ (mA/cm$^2$) |
|---|---|---|
| NCNTs | 203 | 2.9E-02 |
| Au powder | 254 | 7.3E-03 |
| Ag nanoparticles | 220 | 9.7E-03 |

**Table S2.** Free energies of gas phase molecules. Electronic energies are calculated by DFT. A -0.51 eV correction to $E_{ele}$ of CO (g) is included due to the use of PBE functional. Zero point energies are calculated from the vibrational frequencies of the molecules. T is set at 300K, and the entropies are taken from the standard values for $CO_2$, CO and $H_2$ at 1 atm, while that for $H_2O$ is obtained at 0.035 atm.

| **Species** | **$E_{elec}$ (eV)** | **$E_{ZPE}$ (eV)** | **-TS (eV)** | **G (eV)** |
|---|---|---|---|---|
| $CO_2$ (g) | -22.984345 | 0.31 | -0.664733 | -23.339078 |
| CO (g) | -15.304902 (corrected) | 0.1364 | -0.614581 | -16.293083 |
| $H_2O$ (g) | -14.22315 | 0.574445 | -0.65 | -14.298705 |
| $H_2$ (g) | -6.760171 | 0.27714 | -0.40422 | -6.887251 |

**References:**


1. Wu, J., Sharma P. P., Harris B. H., Zhou X.-D. Electrochemical reduction of carbon dioxide: dependence of the Faradaic efficiency and current density on the microstructure and thickness of tin electrode. *J. Power Sources* **258,** 189-194 (2014).

2. Kresse, G., Hafner J. Ab initio molecular dynamics for liquid metals. *Phys. Rev. B* **47,** 558-561 (1993).

3. Kresse, G., Furthmüller J. Efficient iterative schemes for ab initio total-energy calculations using a plane-wave basis set. *Phys. Rev. B* **54,** 11169-11186 (1996).

4. Perdew, J. P., Burke K., Ernzerhof M. Generalized Gradient Approximation Made Simple. *Phys. Rev. Lett.* **77,** 3865-3868 (1996).

5. Nørskov, J. K., Rossmeisl J., Logadottir A., Lindqvist L., Kitchin J. R., Bligaard T.*, et al.* Origin of the Overpotential for Oxygen Reduction at a Fuel-Cell Cathode. *J. Phys. Chem. B* **108,** 17886-17892 (2004).

6. Peterson, A. A., Abild-Pedersen F., Studt F., Rossmeisl J., Norskov J. K. How copper catalyzes the electroreduction of carbon dioxide into hydrocarbon fuels. *Energy. Environ. Sci.* **3,** 1311-1315 (2010).